

DFT calculations have been performed for  $[\text{Fe}(\text{SMe})_4]^{2-}$  and  $[\text{Fe}(\text{SeMe})_4]^{2-}$  in  $C_1$  symmetry. Tables 1a, 1b, 2a and 2b give the charge decompositions for the major spins and minor spins of these systems. Figure 1 gives the MO diagrams of both complexes. Due to spin polarization, the major spin and minor spin levels greatly split in energy.

The highest energy major spin levels of  $[\text{Fe}(\text{SMe})_4]^{2-}$  are therefore of primarily S character and Fe-S antibonding (Table 1a and Figure 1). The lowest energy levels are primarily of Fe-d character and Fe-S bonding. In between is a block of Fe-S orbitals of mixed bonding-antibonding character.

The minor spin level scheme of  $[\text{Fe}(\text{SMe})_4]^{2-}$  exhibits the customary sequence of metal-ligand bonding and antibonding orbitals (Figure 1). The top of the scheme is made up of Fe-S antibonding orbitals (mainly Fe d character, Table 1b). At lower energy follows a block of Fe-S bonding orbitals (mainly S character).

The major and minor spin level schemes of  $[\text{Fe}(\text{SeMe})_4]^{2-}$  (Tables 2a and 2b, respectively) are quite similar. The salient difference between  $[\text{Fe}(\text{SMe})_4]^{2-}$  and  $[\text{Fe}(\text{SeMe})_4]^{2-}$  is the fact that the highest occupied minor spin level has primarily Fe d character in case of  $[\text{Fe}(\text{SMe})_4]^{2-}$  and primarily ligand (Se) character in case of  $[\text{Fe}(\text{SeMe})_4]^{2-}$ . This reflects the higher energy of the Se 4p as compared to the S 3p orbitals. Otherwise, charge decompositions are comparable for both systems, reflecting a similar degree of covalency for the Fe-S and the Fe-Se bond.

**Table 1a.** Major spin charge contribution of  $[\text{Fe(II)(SMe)}_4]^{2-}$  with S=2.

character	label	energy [Hartree]	major spin charge decomposition [%]	
			Fe	S <sup>a</sup>
Fe-S antibonding	41	0.07899	12	77
	40	0.07681	7	80
	39	0.07515	10	77
	38	0.07036	4	84
	37	0.06036	6	78
	36	0.05877	5	78
	35	0.04999	5	75
	34	0.00712	1	69
nonbonding	33	-0.01137	85	6
antibonding	32	-0.03848	44	29
	31	-0.04725	34	32
Fe-S bonding	30	-0.05287	43	29
	29	-0.06865	6	35
	28	-0.07313	55	18
	27	-0.08112	94	3
	26	-0.08556	78	9
	25	-0.08946	80	8

<sup>a</sup> The charge decomposition gives the sum of all contributions of the S atoms.

**Table 1b.** Minor spin charge contribution of  $[\text{Fe(II)(SMe}_4]^{2-}$  with S=2.

character	label	energy [Hartree]	minor spin charge decomposition [%]	
			Fe	S <sup>a</sup>
Fe-S antibonding unoccupied	44	0.26965	62	10
	40	0.23501	32	13
	39	0.22815	40	15
	38	0.22050	75	10
Fe d <sub>z<sup>2</sup></sub> Fe-S π bonding	37	0.07998	59	32
	36	0.07210	3	84
	35	0.07102	7	79
	34	0.06390	7	81
σ bonding	33	0.05759	24	65
	32	0.04483	12	72
	31	0.04362	9	76
	30	0.04218	26	62
S(p)	29	0.01429	0	72
S-Me σ bonding	28	-0.05557	1	43
	27	-0.05746	1	43
	26	-0.05907	3	43
	25	-0.06607	0	39

<sup>a</sup> The charge decomposition gives the sum of all contributions of the S atoms.

**Table 2a.** Major spin charge contribution of  $[\text{Fe(II)}(\text{SeMe})_4]^{2-}$  with S=2.

character	label	energy [Hartree]	major spin charge decomposition [%]	
			Fe	Se <sup>a</sup>
Fe-Se antibonding	41	0.07488	8	80
	40	0.07384	6	83
	39	0.07172	8	79
	38	0.06658	4	87
	37	0.05478	5	80
	36	0.05426	4	79
	35	0.04615	5	76
	34	-0.00152	1	68
non bonding	33	-0.02368	81	8
antibonding	32	-0.04430	24	36
	31	-0.05113	20	35
Fe-Se bonding	30	-0.05708	36	30
	29	-0.06664	3	33
	28	-0.07682	78	8
	27	-0.09222	91	4
	26	-0.09406	93	3
	25	-0.09711	92	3

<sup>a</sup> The charge decomposition gives the sum of all contributions of the Se atoms.

**Table 2b.** Minor spin charge contribution of  $[\text{Fe(II)}(\text{SeMe})_4]^{2-}$  with S=2.

character	label	energy [Hartree]	minor spin charge decomposition [%]	
			Fe	Se <sup>a</sup>
Fe-Se	44	0.25258	59	9
antibonding	40	0.21732	57	16
unoccupied	39	0.21184	57	16
Fe d <sub>z<sup>2</sup></sub>	38	0.20479	80	11
	37	0.07064	20	70
Fe-Se	36	0.06900	5	83
π bonding	35	0.06744	30	59
	34	0.06047	7	82
	33	0.05310	33	58
Fe-Se	32	0.04114	13	73
σ-bonding	31	0.04004	9	76
	30	0.03609	44	46
Se(p)	29	0.00590	0	71
	28	-0.05339	1	42
Se-Me	27	-0.05604	1	41
σ bonding	26	-0.05760	3	42
	25	-0.06398	0	35

<sup>a</sup> The charge decomposition gives the sum of all contributions of the Se atoms.

**Density Functional Theory Calculations.** Spin-unrestricted DFT calculations using Becke's three-parameter hybrid functional with the correlation functional of Lee, Yang and Parr (B3LYP)<sup>1-3</sup> were performed for the quintet ground state ( $S=2$ ) of  $\text{Fe}(\text{SMe})_4^{2-}$  and  $\text{Fe}(\text{SeMe})_4^{2-}$ . The models were optimized in  $C_1$  symmetry, the resulting  $\text{FeS}_4$  and  $\text{FeSe}_4$  units have nearly  $T_d$  symmetry. The LanL2DZ basis set was used for the calculation, which applies Dunning/Huzinaga full double- $\zeta$  (D95) basis functions<sup>4</sup> on the first row and Los Alamos effective core potentials plus DZ functions on all other atoms.<sup>5,6</sup> Convergence was reached when the relative change in the density matrix between subsequent iterations was less than  $1 \times 10^{-8}$  for single points and optimizations. All computational procedures were used as they are implemented in the Gaussian 98 package.<sup>7</sup>

- (1) Becke, A. D. *Phys. Rev. A* **1988**, 38, 3098.
- (2) Becke, A. D. *J. Chem Phys.* **1993**, 98, 1372.
- (3) Becke, A. D. *J. Chem Phys.* **1993**, 98, 5648.
- (4) Dunning, T. H. Jr.; Hay, P. J. in *Modern Theoretical Chemistry* (ed.: H. F. Schaefer III), Plenum, New York, **1976**.
- (5) Hay, P. J.; Wadt, W. R. *J. Chem. Phys.* **1985**, 82, 270 and 299.
- (6) Wadt, W. R.; Hay, P. J. *J. Chem. Phys.* **1985**, 82, 284.
- (7) Frisch, M. J.; Trucks, G. W.; Schlegel, H. B.; Scuseria, G. E.; Robb, M. A.; Cheeseman, J. R.; Zakrzewski, V. G.; Montgomery, J. A., Jr.; Stratmann, R. E.; Burant, J. C.; Dapprich, S.; Millam, J. M.; Daniels, A. D.; Kudin, K. N.; Strain, M. C.; Farkas, O.; Tomasi, J.; Barone, V.; Cossi, M.; Cammi, R.; Mennucci, B.; Pomelli, C.; Adamo, C.; Clifford, S.; Ochterski, J.; Petersson, G. A.; Ayala, P. Y.; Cui, Q.; Morokuma, K.; Salvador, P.; Dannenberg, J. J.; Malick, D. K.; Rabuck, A. D.; Raghavachari, K.; Foresman, J. B.; Cioslowski, J.; Ortiz, J. V.; Baboul, A. G.; Stefanov, B. B.; Liu, G.; Liashenko, A.; Piskorz, P.; Komaromi, I.; Gomperts, R.; Martin, R. L.; Fox, D. J.; Keith, T.; Al-Laham, M. A.; Peng, C. Y.; Nanayakkara, A.; Challacombe, M.; Gill, P. M. W.; Johnson, B.; Chen, W.; Wong, M. W.; Andres, J. L.; Gonzalez, C.; Head-Gordon, M.; Replogle, E. S.; Pople, J. A. Gaussian 98 Rev. A.11; Gaussian, Inc.: Pittsburgh, 2001.

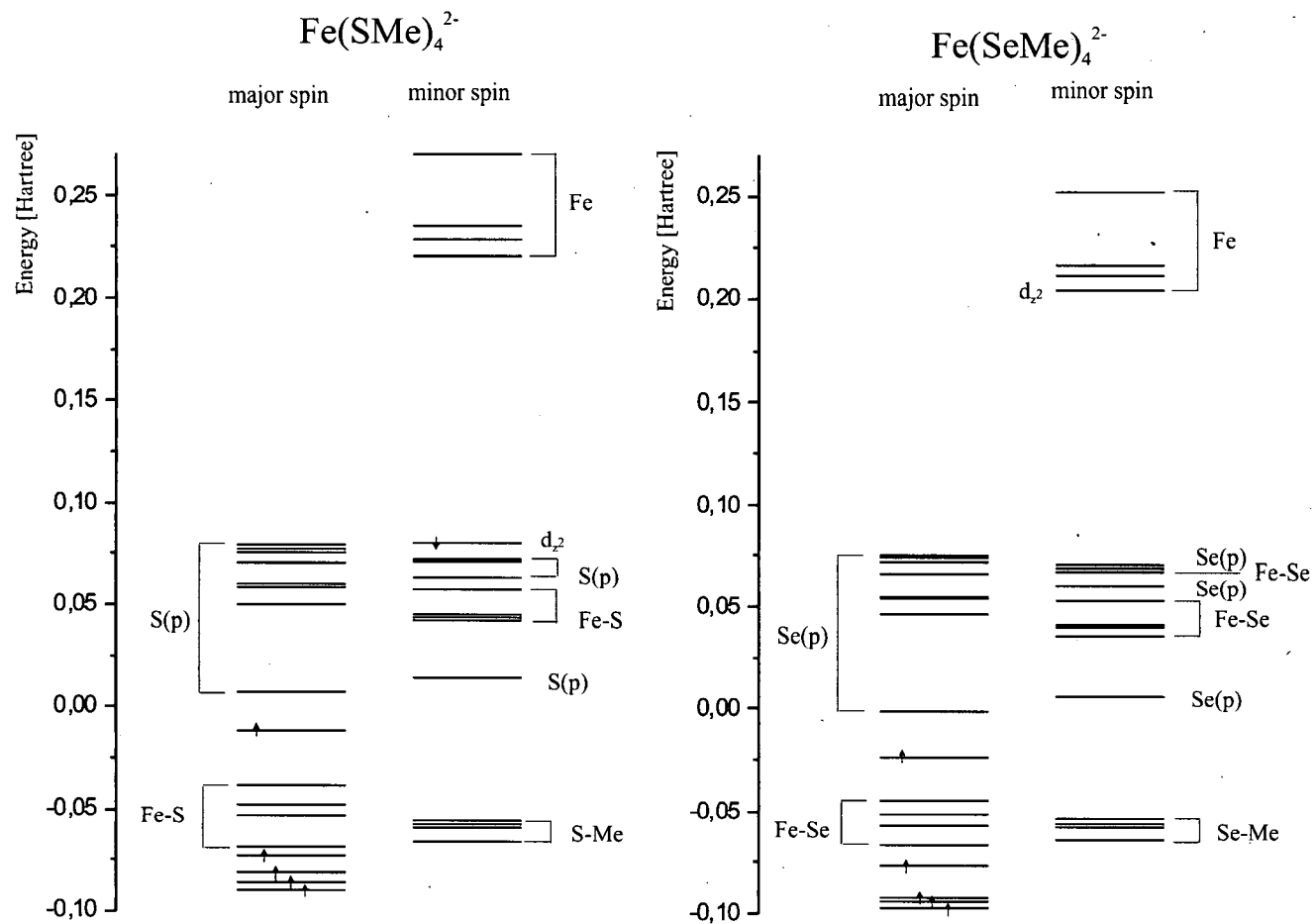


**Figure 1.** MO diagrams of  $\text{Fe}(\text{II})(\text{SMe})_4^{2-}$  and  $\text{Fe}(\text{II})(\text{SeMe})_4^{2-}$ . Both model complexes were optimized in  $C_1$  symmetry with  $S=2$ .

↑ denotes occupied d-orbitals